

Geometry and Statistics of Cosmic Microwave Polarization.

A.D. Dolgov ¹, A.G. Doroshkevich

Theoretical Astrophysics Center

Juliane Maries Vej 30, DK-2100, Copenhagen, Denmark

D.I. Novikov ²

Dept. of Physics and Astronomy, University of Kansas

Lawrence, Kansas, 66045, USA

I.D. Novikov ³

Theoretical Astrophysics Center

Juliane Maries Vej 30, DK-2100, Copenhagen, Denmark

Abstract

Geometrical and statistical properties of polarization of CMB are analyzed. Singular points of the vector field which describes CMB polarization are found and classified. Statistical distribution of the singularities is studied. A possible signature of tensor perturbations in CMB polarization is discussed. For a further analysis of CMB statistics Minkowski functionals are used, which present a technically simple method to search for deviations from a Gaussian distribution.

¹Also: ITEP, Bol. Cheremushkinskaya 25, Moscow 113259, Russia.

² Also: Astro - Space Center of Lebedev Physical Institute, Profsoyuznaya 84/32, Moscow, Russia.

³Also: Astro - Space Center of Lebedev Physical Institute, Profsoyuznaya 84/32, Moscow, Russia; University Observatory, Juliane Maries Vej 30, DK-2100, Copenhagen; NORDITA, Blegdamsvej 17, DK-2100, Copenhagen, Denmark.

1 Introduction

Future high precision measurements of anisotropies of CMB are potentially very powerful tools for cosmological studies. They may present accurate data on the values of the basic cosmological parameters, as well as information about structure formation at an early linear stage. There is a very rich literature on this subject; for a review and a partial list of references see e.g. [1]-[6]. In addition to angular variations of CMB temperature, primordial density fluctuations induce also, as a secondary effect, a polarization of the radiation. A good introduction to the subject can be found in the pioneering papers [7]-[9], while a more up-to-date development is given in refs. [10]-[18]. Our approach here is slightly different from that in the last papers and, though the results mostly coincide or agree, there are some essential differences which we will specify in Secs. 2 and 3 (see also our earlier paper [19]).

Measurements of the polarization of CMB will permit to obtain an additional information which may help to resolve ambiguities in extracting cosmological parameters from the observational data (for a recent discussion of these ambiguities see e.g. ref. [20]). In particular, polarization is quite sensitive to the presence of tensor perturbations (gravitational waves) and, as was shown in refs. [10]-[14] a deviation from zero of the so called pseudoscalar or "magnetic" part of polarization would be unambiguous indication of the presence of gravitational waves. In what follows we will further elaborate this issue and generalize some of the results of ref. [16].

Geometrical properties of polarization field were actively studied in the recent years [13]-[16]. Important features, which characterize geometry and topology of polarization, are the types of singularities of the vector flux lines tangent to the direction of maximum polarization [19] (for an earlier paper see ref. [21]). This vector

is parallel to one of the eigenvectors of the Stokes matrix and have the magnitude equal to the magnitude of polarization. The points where this vector vanishes, so that no direction is determined, are singular points on the polarization map and the character of the singularity to a large extent determines the relief of the polarization map, even rather away from the points of vanishing polarization. The maps simulated in different papers, including ours (see Fig. 4), demonstrate that the behavior (topology) of the flux lines of the polarization field at the points where polarization is non-vanishing, is determined by the type of the singularity at vanishing polarization. Hence one may make a conclusion about the types of the singular points studying polarization maps in the regions where polarization is measurable. The properties of these singular points are discussed in detail in Secs. 4 and 5.

Statistical properties of the anisotropy of CMB temperature and CMB polarization are of primary importance for an understanding of their origin. At the present day only two mechanisms of generation of primordial density perturbations are known: inflation and topological defects. Simplest inflationary scenarios predict Gaussian perturbations that results in the Gaussianity of the CMB temperature fluctuations and polarization at the surface of last scattering. Tests of a Gaussian nature of the temperature fluctuations of CMB, together with a study of its polarization, are important probes of inflation. A possible method of testing a Gaussianity of CMB is a study of statistics of the singular points discussed in Sec. 4.4. The same statistical tests may also be useful for discrimination of signal from noise because Gaussian distributions of both temperature fluctuation and polarization generated by noise are rather improbable.

Statistics of global geometrical properties of CMB maps, both for temperature fluctuations and polarization, can be efficiently studied with Minkowski Functionals

(MF) [22, 23]. Applications of this approach to the temperature fluctuations and to polarization has been discussed in refs. [24]-[26] and refs. [21, 19], respectively. In a recent paper [27] genus statistic of simulated polarization maps was analyzed. In Sec. 6 we apply all three MF's, which are known for two dimensional maps, for the study of statistical properties of CMB polarization.

This paper is organized as follow: The basic concepts and notations are introduced in Sec. 2. In Sec. 3 a local description of polarization is compared with a nonlocal one. In Secs. 4 and 5 the classification of singular points is discussed and various approaches to this problem are compared. The properties of Minkowski Functionals are considered in Sec. 6. We finish with Sec. 7 where a short discussion of results can be found.

2 Generalities

Here we will describe some general properties of CMB polarization and present the necessary formalism. This section has an introductory character and to some extent is described in the literature. We make a simplifying assumption that the relevant angular scales are sufficiently small, so that the corresponding part on the sky is almost flat. In this approximation the polarization field on the sky can be considered as two dimensional field on flat (x, y) -plane. The photon polarization is described by the second rank tensor a_{ij} in the plane perpendicular to the photon propagation. By definition this tensor is traceless, because the trace part, proportional to unit matrix, corresponds to zero polarization and can be absorbed in the total intensity of radiation. It is convenient to expand this tensor in terms of the Pauli matrices σ_α ,

$\alpha = 1, 2, 3$, which form a complete system in 2×2 traceless matrix space:

$$\mathbf{a} = \xi_\alpha \sigma_\alpha \quad (1)$$

The parameter ξ_2 is equal to the amplitude of circular polarization, which is not generated by Thomson scattering (due to parity conservation), so that it is assumed usually that $\xi_2 = 0$. In this case the matrix \mathbf{a} is symmetric and is determined by two functions:

$$\mathbf{a} = \begin{pmatrix} Q & U \\ U & -Q \end{pmatrix} \quad (2)$$

The functions Q and U depend upon the coordinate frame; they are components of the tensor a_{ij} and obey the corresponding tensor transformation law:

$$a'_{ij} = T_i^k T_j^l a_{kl} \quad (3)$$

where the coordinate transformation is given by $x'_i = T_i^k x_k$. In particular under rotation of the coordinate system with

$$\mathbf{T} = \begin{pmatrix} c & s \\ -s & c \end{pmatrix} \quad (4)$$

where $c = \cos \phi$, $s = \sin \phi$, and ϕ is the rotation angle, the parameters Q and U are transformed as:

$$\begin{aligned} Q' &= Q \cos 2\phi + U \sin 2\phi \\ U' &= -Q \sin 2\phi + U \cos 2\phi \end{aligned} \quad (5)$$

It is more convenient in many cases to work with invariant quantities or at least with vector ones, whose direction on the polarization map is easy to visualize. There are

the following invariants (or what is the same, scalars) that may be constructed from the second rank tensor. First, of course, it is the trace, $\text{Tr } \mathbf{a} = a_{ii}$. In the considered case it is zero. The second invariant is the determinant of the matrix \mathbf{a} ,

$$\det \mathbf{a} = Q^2 + U^2 \quad (6)$$

The maximum magnitude of polarization is given by $\sqrt{Q^2 + U^2}$. The direction of maximum polarization is determined by one of the eigenvectors of the matrix a_{ij} (see e.g. ref. [19]).

These are the well known algebraic invariants which exist in any space dimensions. One may construct two more invariants, using vector operator of differentiation. They can be chosen as:

$$\begin{aligned} S &= \partial_i \partial_j a_{ij} \\ P &= \epsilon_{kj} \partial_k \partial_i a_{ij} \end{aligned} \quad (7)$$

where $j = 1, 2$ and $\partial_j = \partial / \partial x^j$. In terms of Q and U these invariants are expressed as:

$$\begin{aligned} S &= (\partial_1^2 - \partial_2^2)Q + 2\partial_1 \partial_2 U \\ P &= (\partial_1^2 - \partial_2^2)U - 2\partial_1 \partial_2 Q \end{aligned} \quad (8)$$

The first scalar invariant exists in any space dimension, while the second pseudo-scalar one exists only in two dimensional space, because of the presence of antisymmetric pseudo-tensor ϵ_{kj} (analogous antisymmetric tensor in higher dimensions D has D indices). These quantities S and P coincide, up to a scalar factor, with the introduced in refs. [10, 12] B and E fields. To our opinion it is more natural to denote them as S and P to stress their scalar and pseudo-scalar nature and not as electric and magnetic

parts of polarization because these quantities have nothing to do with vectors. In this sense we agree with the terminology of ref. [28] (see also [13, 15]).

An important feature of the pseudo-scalar P is that it vanishes if only scalar perturbations induces polarization in CMB. In this case the Stokes matrix can be written in terms of derivatives of one scalar function:

$$a_{ij} = (2\partial_i\partial_j - \delta_{ij}\partial_k\partial_k)\Psi \quad (9)$$

It is straightforward to check that indeed $P = 0$. We do not share the opinion and/or terminology of refs. [14, 17] where it is stated that the corresponding field does not possess a curl. As has been shown in ref. [19] this is not true and generically the eigenvectors of the Stokes matrix are not curless. The validity of this general statement can be verified on simple examples. It means in particular that the flux lines of the direction of maximum polarization may have a nonzero vorticity in contrast to the statement of refs. [14, 17].

If tensor perturbations are non-vanishing, the polarization matrix has the general form determined by two independent functions. As is well known, an arbitrary three dimensional vector can be expanded in terms of scalar and vector potentials as

$$\vec{V} = \text{grad } \Phi + \text{curl } \vec{A} \quad (10)$$

In two dimensions an arbitrary vector can be expressed as derivatives of a scalar and a pseudoscalar:

$$V_j = \partial_j\Phi_1 + \epsilon_{jk}\partial_k\Phi_2 \quad (11)$$

In direct analogy to that, an arbitrary traceless symmetric 2×2 -matrix can be presented in terms of scalar and pseudo-scalar potentials as:

$$a_{ij} = (2\partial_i\partial_j - \delta_{ij}\partial^2)\Psi + (\epsilon_{ik}\partial_k\partial_j + \epsilon_{jk}\partial_k\partial_i)\Phi \quad (12)$$

Of course now the pseudo-scalar P defined in eq. (7) does not vanish and this property permits to observe possible tensor perturbations by measurement of CMB polarization [10]-[16]. If $\Psi = 0$ then the scalar S vanishes. Unfortunately it would not mean that tensor perturbations dominate because they contribute both into Φ and Ψ .

3 Local and nonlocal description of polarization

It is an interesting observational problem which quantity is easier to measure in a noisy background, a differential local or an integrated global one. As was stated in ref. [15] a measurement of an integrated quantity would be much more robust. And correspondingly the field variables S and P (or in notations of papers [10]-[12], E and B) were expressed as integrals over all or a part of the sky. We think that the answer to the question on the best observational strategy very much depends on the properties of the noise. For example if the noise in polarization field of CMB is created by point-like sources, chaotically distributed on the sky with the mean separation larger than the resolution of the antenna, then the measurement of local differential quantities, as e.g. direct measurements of S and P given by eq. (7) seems easier. However there may be sources of the noise that would be easier to suppress if one measures a quantity which is averaged over whole (which is not possible) or a part of the sky. To this end we re-derive the expressions for integrated S and P (or E and B) presented in ref. [16]. The derivation is presented in great detail because of some disagreement with ref. [16]. The results are very close but we show that the window function may have a more general form even for the same choice of normalization function $N(l^2)$, defined below.

Let us first define the Fourier transformed fields:

$$\tilde{Q}(\vec{l}) = \int d^2y e^{-i\vec{l}\vec{y}} Q(\vec{y}) \quad (13)$$

and the similar one for U . The Fourier transformed scalar and pseudo-scalar fields can be written as

$$\begin{aligned} \tilde{S}_N(\vec{l}) &= N(l^2) \int d^2y e^{-i\vec{l}\vec{y}} [Q(\vec{y}) \cos 2\phi_l + U(\vec{y}) \sin 2\phi_l] \\ \tilde{P}_N(\vec{l}) &= N(l^2) \int d^2y e^{-i\vec{l}\vec{y}} [U(\vec{y}) \cos 2\phi_l - Q(\vec{y}) \sin 2\phi_l] \end{aligned} \quad (14)$$

where ϕ_l is the polar angle in the plane of Fourier coordinates \vec{l} . The scalar function $N(l^2)$ is arbitrary. It preserves scalar or pseudo-scalar property of S and P . For the definition (7) one has to choose $N(l^2) = l^2$. The definition used in ref. [16] is $N(l^2) = 1$. This means that a non-locality is introduced in the coordinate space by the inverse Laplace operator, $1/\partial^2$, that is by the Green's function of the Laplacian.

Now we can make the inverse Fourier transform to obtain the functions S_N and P_N in coordinate space:

$$\begin{aligned} S_N(\vec{x}) &= \int \frac{d^2l}{(2\pi)^2} N(l^2) \int d^2y e^{i\vec{l}(\vec{x}-\vec{y})} [Q(\vec{y}) \cos 2\phi_l + U(\vec{y}) \sin 2\phi_l] \\ P_N(\vec{x}) &= \int \frac{d^2l}{(2\pi)^2} N(l^2) \int d^2y e^{i\vec{l}(\vec{x}-\vec{y})} [-Q(\vec{y}) \sin 2\phi_l + U(\vec{y}) \cos 2\phi_l] \end{aligned} \quad (15)$$

where ϕ_l is the angle between the vector \vec{l} and some fixed direction; it is convenient to choose the latter as the direction of vector \vec{x} , so that $\phi_l \equiv \phi_{xl}$.

Integration over directions of vector \vec{l} can be done explicitly. To simplify the notations let us introduce

$$\vec{\rho} = \vec{x} - \vec{y} \quad (16)$$

and three angles $\phi_{l\rho}$, $\phi_{\rho x}$, and ϕ_{xl} between the directions of the indicated vectors. Evidently

$$\phi_{l\rho} + \phi_{\rho x} + \phi_{xl} = 0 \quad (17)$$

The angular integral is reduced to

$$\int_0^{2\pi} d\phi_{l\rho} e^{il\rho \cos \phi_{l\rho}} (A \cos 2\phi_{l\rho} + B \sin 2\phi_{l\rho}) \quad (18)$$

where the coefficient functions A and B do not depend on $\phi_{l\rho}$. The second term vanishes, while the first one gives

$$\int_0^{2\pi} d\phi_{l\rho} e^{il\rho \cos \phi_{l\rho}} \cos 2\phi_{l\rho} = -2\pi J_2(l\rho) \quad (19)$$

where $J_2(z)$ is the Bessel function (see e.g. [29]).

The integration over magnitude of l depends upon the form of the function $N(l^2)$ and the result is a function of the magnitude of the vector $\vec{\rho}$:

$$\int_0^\infty dl l N(l^2) J_2(l\rho) = F_N(\rho) \quad (20)$$

For the particular case of $N(l^2) = 1$ chosen in ref. [16] the integral can be taken as follows. It is formally divergent so some regularization procedure should be applied. This can be achieved by introducing a small imaginary part to l to ensure convergence (in other words, we have to shift the contour of integration to the upper l -half-plane). Using the relation [29]:

$$z J_2(z) = J_1(z) - z J_1'(z) \quad (21)$$

and integrating by parts, we obtain:

$$F_1(\rho) = \frac{1}{\rho^2} \int_0^\infty dz z J_2(z) = \frac{1}{\rho^2} \left[2 \int_0^\infty dz J_1(z) - z J_1(z) \Big|_0^\infty \right] = \frac{2}{\rho^2} \quad (22)$$

Now taking all the contributions together we obtain:

$$\begin{aligned}
S_N(\vec{x}) &= \frac{1}{2\pi} \int_0^\infty d\rho \rho F_N(\rho) \int_0^{2\pi} d\phi [Q(\vec{x} - \vec{\rho}) \cos 2\phi + U(\vec{x} - \vec{\rho}) \sin 2\phi] \\
P_N(\vec{x}) &= \frac{1}{2\pi} \int_0^\infty d\rho \rho F_N(\rho) \int_0^{2\pi} d\phi [-Q(\vec{x} - \vec{\rho}) \sin 2\phi + U(\vec{x} - \vec{\rho}) \cos 2\phi]
\end{aligned} \tag{23}$$

For the particular case of $F_N(\rho) = F_1(\rho) = 2/\rho^2$ considered in ref. [16] we obtain almost the same result as the quoted paper with the only difference that we do not see any reason to assume that the window function $F_1(\rho) = 2/\rho^2$ should be taken zero at $\rho = 0$. Anyhow, this difference has zero measure and does not have any impact on the value of the integrals (23). Hence it may be disregarded. What, as we think, is more essential is the statement of ref. [16] that in order to avoid difficult (or even impossible) integration of the data over the whole sky one may use a modified window function:

$$F_{sz}(\rho) = -g(\rho) + \frac{2}{\rho^2} \int_0^\rho d\rho' \rho' g(\rho') \tag{24}$$

with the function $g(\rho)$ subject to the condition:

$$\int d\rho \rho g(\rho) = 0 \tag{25}$$

where the last integral is taken over all the sky.

We believe that any window function can be used and no additional conditions are necessary. To show that we calculate the functions $S_N(\vec{x})$ and $P_N(\vec{x})$ for the particular case of scalar perturbations when the Stokes matrix is given by expression (9). Calculation of derivatives in polar coordinates is straightforward and after some algebra we obtain:

$$\begin{aligned}
S_N(\vec{x}) &= \frac{1}{2\pi} \int_0^\infty d\rho \rho W(\rho) \int_0^{2\pi} d\phi \left(\Psi_{\rho,\rho}(\vec{x} - \vec{\rho}) - \frac{\Psi_\rho(\vec{x} - \vec{\rho})}{\rho} \right) \\
P_N(\vec{x}) &= \frac{1}{2\pi} \int_0^\infty d\rho \rho W(\rho) \int_0^{2\pi} d\phi \left(\frac{2\Psi_{\rho,\phi}(\vec{x} - \vec{\rho})}{\rho} - \frac{2\Psi_\phi(\vec{x} - \vec{\rho})}{\rho^2} \right)
\end{aligned} \tag{26}$$

where sub- ρ or sub- ϕ means differentiation with respect to the corresponding variable and $W(\rho)$ is an arbitrary window function.

One can see from the second of these expressions that indeed P vanishes for any window function. Thus to prove the absence of tensor perturbations, one should either observe vanishing of the local quantity $P(\vec{x})$ given by eq. (8) or of the nonlocal one given by eq. (26) with an arbitrary convenient window function $W(\rho)$. Which method would be more efficient depends upon the properties of the noise.

4 Singular points in polarization maps

4.1 Introductory remarks

Polarization state of photons of CMB can be described by the direction of maximum polarization and its magnitude; the former is parallel to the eigen-vector of the Stokes matrix and the latter is equal to $\sqrt{Q^2 + U^2}$. Polarization maps simulated in different papers present the corresponding vector field on two-dimensional plane. For the analysis of the flux lines on this map it is very important to know the properties of the singular points of this vector field. It has been done in ref. [19] (see also [21]). Another approach was taken in refs [15, 16] where the properties of the flux lines were analyzed in terms of basis functions of tensor spherical harmonics (see figs. 1 in refs. [15, 16]). However the flux lines of these basic functions are quite different from the behavior of the flux lines of the polarization vector. Of course the analysis in terms of tensor harmonics and the behavior of Stokes parameters Q and U can be used for description of polarization maps but the analysis in terms of eigenvectors of the Stokes matrix permits to make a more direct description of the properties of the polarization field. Possible types of different singular points as well as their statistical

distributions may bring a new piece of information about properties of CMB. Of course a measurement of CMB polarization near the point where it vanishes is a very difficult observational problem. However it is not necessary to go exactly to the point where $Q^2 + U^2 = 0$. The type of the singularity can be determined by the pattern created by the flux lines in the region where polarization is non-vanishing (see an example of simulated polarization map below in Fig. 4).

The analysis of singular points of the polarization vector field was performed in ref. [19] and [21]. It was found in [19] that their types do not fit the well known classification of singular points of vector fields in the standard theory of dynamical systems. Due to non-analytic behavior of the eigen-vectors near the the zero points, $Q^2 + U^2 = 0$, the separatrices end at the singularity, while in the usual case they smoothly continue through these points. These unusual behavior, found in our paper [19], is well observed in the polarization maps simulated in refs. [16] and in the maps of our paper below(Figs. 4,5). In this and the next section we present a further development of the analysis of our previous shorter paper [19].

4.2 Basic equations

The eigenvectors of polarization matrix (2) are:

$$\begin{aligned}\vec{n}^+ &\sim \{U, \lambda - Q\} \\ \vec{n}^- &\sim \{-U, \lambda + Q\}\end{aligned}\tag{27}$$

where $\lambda = \sqrt{Q^2 + U^2}$ is the magnitude of the eigenvalue and the vectors \vec{n}^\pm correspond respectively to the positive and negative eigenvalues, $\pm\lambda$. The vector \vec{n}^+ is parallel to the direction of the maximum polarization, while \vec{n}^- goes along the direction of the minimal polarization. This is evident in the basis of eigenvectors where

the polarization matrix is diagonal, $\mathbf{a} = \text{diag}\{\lambda, -\lambda\}$. The total intensity of light polarized along \vec{n}^\pm is given by $I_\pm = I_0 \pm \lambda$. Thus the intensity along \vec{n}^+ is bigger.

For definiteness we will consider the field of directions of the vector \vec{n}^+ and the singular points in this field. The problem of singular points of a vector field \vec{V} is investigated for the case when the direction of this two-dimensional vector field with the components $[x(t), y(t)]$ is governed by the equation

$$\frac{dy}{dx} = \frac{F_1(x, y)}{F_2(x, y)} \quad (28)$$

Singularities may appear if simultaneously both functions $F_{1,2}(x, y)$ vanish. In this case the conditions of uniqueness of the solution of the differential equation is not fulfilled and more than one integral curve may pass through the same point. The standard theory is developed for the case when the functions $F_{1,2}$ are analytic near these zeroes, and their first order Taylor expansion has the form:

$$F_j = a_j(x - x_0) + b_j(y - y_0) \quad (29)$$

The following three singular points are possible in this case: knots, saddles, and foci (see e.g. [30]). The separatrices of the solutions are two intersecting lines, which are simply straight lines in the linear approximation.

However in the case of polarization vector field the basic equation has the form:

$$\frac{dy}{dx} = \frac{n_y^+}{n_x^+} = \frac{\lambda - Q}{U} \quad (30)$$

The singular points may appear, as above, if both numerator and denominator vanish. It is equivalent to the condition $Q = U = 0$. An essential difference to the standard case is that now the numerator is not analytic near zero. This fact results in a quite different behavior of the integral curves near these points. The standard theory is not

applicable to this case and below we will investigate the structure of solutions in the vicinity of these points directly. We assume that the functions Q and U are analytic near the points where $Q = U = 0$, so that they can be expanded as:

$$\begin{aligned} Q &\approx q_1x + q_2y \\ U &\approx u_1x + u_2y \end{aligned} \tag{31}$$

For the sake of brevity we assume that Q and U vanish at $x = y = 0$.

4.3 Types of singular points

It is convenient to introduce the new coordinates:

$$\begin{aligned} \xi &= q_1x + q_2y \\ \eta &= u_1x + u_2y \end{aligned} \tag{32}$$

Since this coordinate transformation corresponds to a rotation and rescaling of the coordinates, the forms of singular points would remain the same. Now we introduce polar coordinates on the plane (ξ, η) :

$$\xi = r \cos \phi, \quad \eta = r \sin \phi \tag{33}$$

In these coordinates the equation (30) is rewritten as

$$\frac{d \ln r}{d\phi} = \frac{N}{D} \equiv \frac{q_2t^3 + (q_1 - 2u_2)t^2 - (q_2 + 2u_1)t - q_1}{u_2t^3 + (u_1 + 2q_2)t^2 + (2q_1 - u_2)t - u_1} \tag{34}$$

where $t = \tan(\phi/2)$.

In the general case the denominator D has three roots t_j , $j = 1, 2, 3$. Without loss of generality we may assume that $u_2 = 1$. Then these roots satisfy the conditions:

$$t_1t_2t_3 = u_1,$$

$$\begin{aligned}
t_1 t_2 + t_2 t_3 + t_3 t_1 &= 2q_1 - 1, \\
t_1 + t_2 + t_3 &= -(u_1 + 2q_2)
\end{aligned}
\tag{35}$$

The integration of equation (34) becomes straightforward if we expand the r.h.s. in elementary fractions:

$$\frac{d \ln r}{d\phi} = q_1 + \sum_j^3 \frac{B_j}{t - t_j}
\tag{36}$$

where, as one can easily see, $B_j = N(t_j)/(t_j - t_k)(t_j - t_l)$, none of j, k, l are equal to any of the others. It is straightforward to verify that

$$B_1 = -\frac{(1 + t_2 t_3)(1 + t_1^2)^2}{2(t_1 - t_2)(t_1 - t_3)}
\tag{37}$$

Remaining parameters B_2 and B_3 are obtained by cyclic permutations.

Since $d \ln r / d\phi = (d \ln r / dt)(1 + t^2)/2$ the equation can be finally rewritten as

$$\frac{d \ln r}{dt} = \frac{2}{1 + t^2} \left(q_1 + \sum_j^3 \frac{B_j}{t - t_j} \right)
\tag{38}$$

and the integration becomes straightforward. The corresponding solution is:

$$r = r_0 (1 + t^2) \prod_j^3 (t - t_j)^{2\nu_j}
\tag{39}$$

where r_0 is an arbitrary constant and the powers ν_j are

$$\nu_j = \frac{B_j}{1 + t_j^2}
\tag{40}$$

with the constants B_j given by eq. (37). It can be checked that ν_j satisfy the following conditions:

$$\sum_j^3 \nu_j = -1,
\tag{41}$$

$$\sum_j^3 \nu_j t_j = -\frac{1}{2} \left(\sum_j^3 t_j + \prod_j^3 t_j \right) = q_1, \quad (42)$$

$$\prod_j^3 \nu_j = \frac{(1+t_1^2)(1+t_2^2)(1+t_3^2)}{8(t_1-t_2)^2(t_2-t_3)^2(t_3-t_1)^2} (1+t_1 t_2)(1+t_2 t_3)(1+t_3 t_1) \quad (43)$$

The last three factors in equation (43) are proportional to the determinant $d = q_1 u_2 - q_2 u_1$:

$$(1+t_1 t_2)(1+t_2 t_3)(1+t_3 t_1) = 2(q_1 u_2 - u_1 q_2)/u_2^2 \equiv 2d/u_2^2 \quad (44)$$

If all the roots t_j are real, then the sign of the product $\prod_j^3 \nu_j$ is the same as the sign of the determinant d . If however one of the roots, e.g. t_1 , is real and the other two are complex conjugate, the sign of the determinant and of the product (43) are opposite.

Now we can make the classification of the singular points. Let us first consider the case when all the roots t_j are real. The behavior of the solution is determined by the signs of the powers ν_j . Due to equation (41) at least one of the powers ν_j must be negative. To see what other signs are possible let us assume (without loss of generality) that

$$t_1 > t_2 > t_3 \quad (45)$$

In this case the following sign relations are valid:

$$\begin{aligned} \text{sign}[\nu_1] &= \text{sign}[-(1+t_2 t_3)], \\ \text{sign}[\nu_2] &= \text{sign}[(1+t_1 t_3)], \\ \text{sign}[\nu_3] &= \text{sign}[-(1+t_1 t_2)] \end{aligned} \quad (46)$$

If e.g. $t_3 > 0$, the following signs of ν_j are realized $(-, +, -)$. If $t_3 < 0$ but $t_2 > 0$, then $\nu_3 < 0$ and one or both ν_1 and ν_2 are negative. They cannot both be positive

because if $(1 + t_1 t_3) > 0$, then $(1 + t_2 t_3) > 0$ too and $\nu_1 < 0$. Analogously, in the case $t_1 > 0$ and $t_2 < 0$ the set of signs $(-, +, +)$ for any sequence of ν_j is impossible. In the case when all t_j are negative, the sign pattern is $(-, +, -)$. Thus only two sign combinations for ν_j are possible: $(-, -, -)$ and $(-, -, +)$. The first one is realized when $d < 0$ in accordance with expressions (43) and (44). If the determinant is positive, then the signs of ν_j are $(-, -, +)$.

In the case when $d < 0$ the solution does not pass through zero in the vicinity of the singular point. Its behavior is similar to the usual saddle with the only difference that there are three and not four, as in the usual case, linear asymptotes/separatrices (see Fig. 1a). We will also call it a "saddle". The fact that in our case separatrices are not continued through the singular point, in contrast to the usual singularities is related to the non-analytic behavior of the equation (30) due to the square root singularity.

If $d > 0$, then the sign pattern is $(-, -, +)$ and the solution vanishes along one of the directions and tends to infinity along the other two. The form of the solution is quite different from the standard ones. The field line cannot be continued along $\phi = \phi_1$ into $\phi = \phi_1 + \pi$ as can be done in the usual case. We will call this type of singularity a "beak" (see Fig. 1b).

If only one of the roots t_j is real and the other two are complex conjugate, the solution has the form:

$$\frac{r}{r_0} = (t^2 + 1) |t - t_2|^{4\text{Re}\nu_2} \exp(4\beta \text{Im}\nu_2) (t - t_1)^{2\nu_1} \quad (47)$$

where $\beta = \tan^{-1}[\text{Im}t_2/(t - \text{Re}t_2)]$. The real root ν_1 is negative, as is seen from eq. (43) and thus r does not vanish in vicinity of such singular point. The flux lines of the polarization field for this case are presented in Fig. 1c. This type of singularity

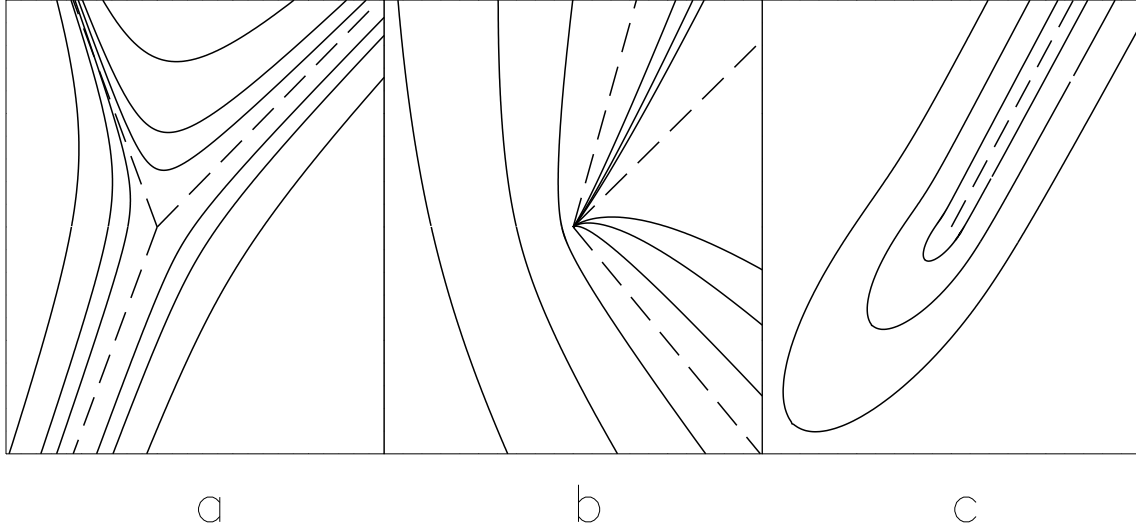


Figure 1: Flux lines for three different types of singular points: (a) saddle, (b) beak, and (c) comet. Dashed lines show peculiar solutions (separatrices).

can be called a "comet". This case is realized when determinant d is positive.

4.4 Probabilities of various types of singularities

The relative weights of different singular points was calculated in the following way. It is evident that the probability of "saddles" is 50% because saddles appears if and only if $d < 0$. The probability of comets and beaks was found numerically from the conditions that $d > 0$ and there is a single real root of the equation $D = 0$ (for comets) or there are three real roots (for beaks), where D is the denominator in the expression (34). The probability of appearance of saddles, beaks and comets for random choice of q_1 , q_2 , u_1 , and u_2 , is correspondingly $W_s = 0.500$, $W_b \approx 0.116$, $W_c \approx 0.384$.

One can also estimate the number density of the singular points in the following way (see e.g. [9, 21]). All singular points correspond to the case when both $Q = 0$

and $U = 0$. The number density of these points is proportional to

$$dQdU = |d|dxdy \tag{48}$$

and thus the density is given by the average value of the determinate, $d = q_1u_2 - q_2u_1$. It can be shown that saddles make 50% of all singular points $\langle n_s \rangle = 0.5\langle n \rangle$, where n is the number density of all singular points. Calculations of the number density of beaks and comets are more complicated and should be done numerically. According to our estimates the surface densities for beaks and comets are correspondingly $\langle n_b \rangle \approx 0.052\langle n \rangle$ and $\langle n_c \rangle \approx 0.448\langle n \rangle$. Deviations from these and above found numbers for $W_{s,b,c}$ may signal deviations from Gaussian nature of perturbations.

5 Comparison of two classification methods

As we have mentioned above the first classification of singular points in CMB polarization map was performed in ref. [21], where the equation

$$\frac{dy}{dx} = \frac{Q}{U} \tag{49}$$

was used to describe the behavior of the flux lines of the "vector" $\vec{V} = [U, Q]$. However under coordinate transformations U and Q are not transformed as components of a vector but as components of a second rank tensor in accordance with eq. (5). Because of that the maps of the flux lines of the "vector" \vec{V} would not be invariant with respect to rotation of the coordinate system. In a fixed reference frame there could be three possible types of singular points in accordance with the standard classification [30]: knots, foci, and saddles. This is so because both functions Q and U generically should be analytic near the point where both of them vanish. The types of singularities in these classification scheme depend in particular upon the sign of the determinant

$d = q_1 u_2 - q_2 u_1$ introduced above. If $d > 0$, then the singular points are saddles, while for $d < 0$ there may be both foci and knots.

It can be shown that d is invariant under coordinate rotation. Thus saddles retain their identity in different coordinate frame. On the other hand, foci and knots may transform into each other under rotation. So the topology of the map of flux lines of the "vector" \vec{V} would look differently in different coordinate systems, though the positions of the singular points evidently remains the same. Moreover the flux lines of another possible "vector", $\vec{W} = [Q, U]$ are in a sense complementary to those of \vec{V} . The relevant determinant changes sign and thus saddles of \vec{V} correspond to foci and knots of \vec{W} and vice versa.

In contrast to classification based on \vec{V} or \vec{W} , the description of the polarization map in terms of eigenvectors of the Stokes matrix, considered in the previous sections and in ref. [19], is invariant with respect to coordinate transformations, so that types of the singular points do not change under rotation. As we have argued in the previous section, positive d gives rise to either to beaks or comets, while negative d could produce only saddles. Thus a saddle in the flux lines of $\vec{n}^{(+)}$ corresponds to a knot or a focus on \vec{V} -map and to a saddle on \vec{W} -map. A comet or a beak on $\vec{n}^{(+)}$ -map both correspond to a saddle on \vec{V} -map or to either a knot or a focus on \vec{W} -map. The latter relations may be different in different coordinate frames because, as we mentioned above, knots and foci transforms into each other under rotation, while beaks and comets remain the same (this is also true for saddles on $\vec{n}^{(+)}$ -map). These statements are illustrated on Figs. 1-3 where examples of the maps for $\vec{n}^{(+)}$ and for \vec{V} are presented.

The simulated 500*500 pixels, $5^\circ \times 5^\circ$ degree map of the CMB polarization field for the Standard CDM model with the HWFM resolution 0.3° is presented in Fig.4. Each

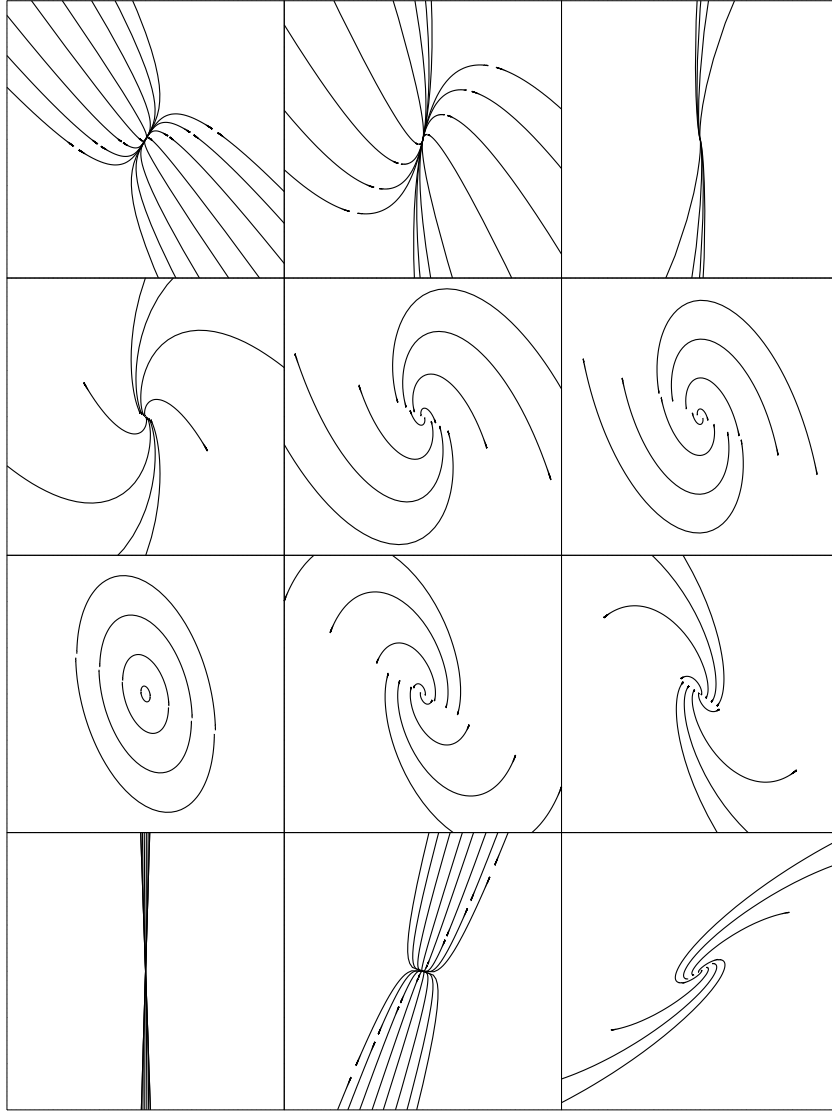


Figure 2: Transformation of the flux lines of "vector" \vec{V} due to rotation of coordinates near the saddle type singularity of $\vec{n}^{(+)}$, plotted in Fig. 1(a). The set of maps from left to right and from the top to the bottom corresponds to rotations with respect to the first one by the angles: $\phi = 5^\circ, 10^\circ, 15^\circ, 20^\circ, 22.5^\circ, 25.6^\circ, 30^\circ, 34^\circ, 49^\circ, 57^\circ$, and 70° .

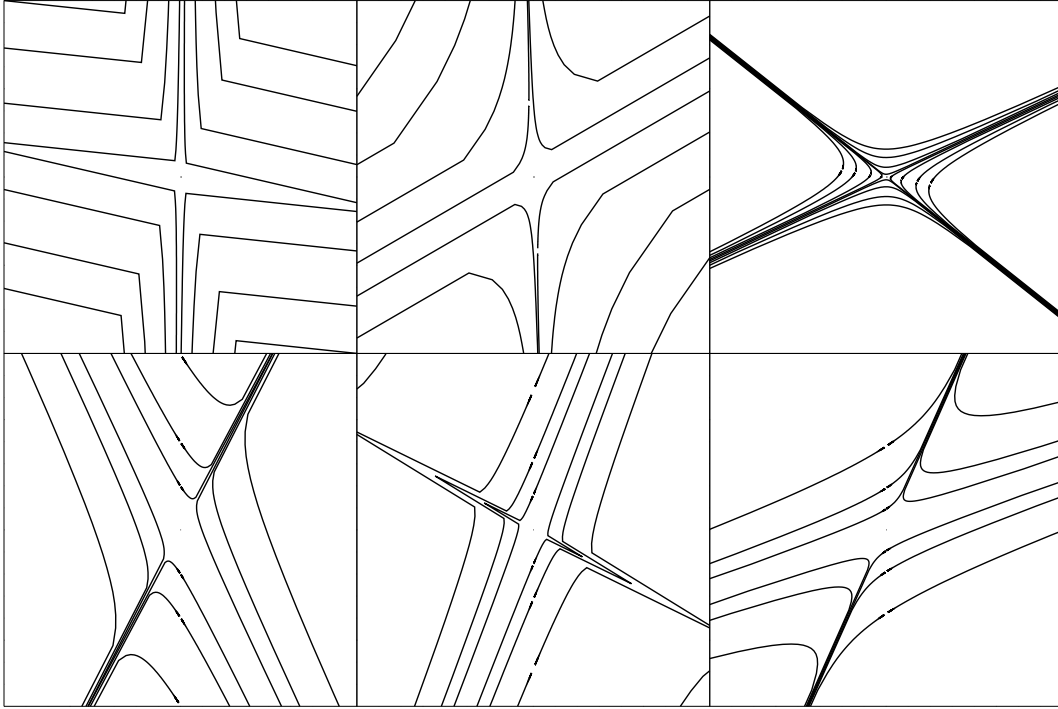


Figure 3: Transformation of the flux lines of the "vector" V near the beak (upper panel) and comet (lower panel) type singularities of $\vec{n}^{(+)}$, plotted in Fig. 1(b) and 1(c) respectively. The maps from left to right correspond to rotation by $\phi = 45^\circ$ and 90° with respect to the first one.

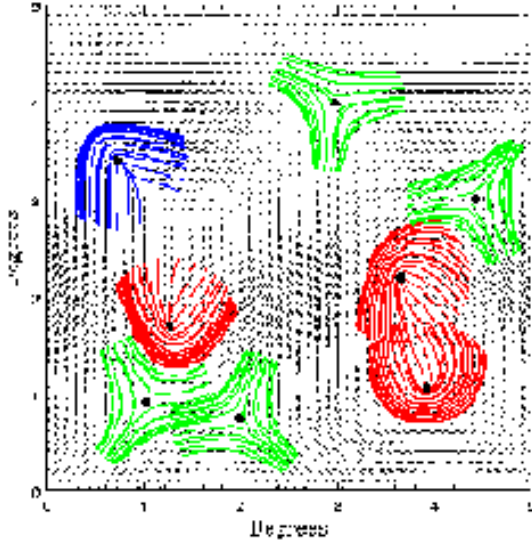


Figure 4: Simulated map of CMB polarization vector field $\vec{n}^{(+)}$ (see Sec. 5 for details). Solid lines show the flux line behavior near singular points where polarization vanishes.

vector represents orientation of the linear polarization with the angle $\frac{1}{2}\tan^{-1}(U/Q)$ counterclockwise to the positive direction of the X axes. Length of each vector is proportional to $\sqrt{Q^2 + U^2}$. For visual clarity we use only 50*50 pixels. Solid lines represent the behavior of the field in the vicinity of non-polarized points. In this picture we have 4 saddles, 3 comets and 1 beak. For comparison of two approaches described in this section the same random Gaussian realization as for Fig. 4 but for the pseudo vector \vec{V} is presented in Fig. 5. As we discussed above the types of the singularities in this case are different. There are 4 saddles which correspond to comets or beaks in the polarization map of Fig. 4 as well as 2 knots and 2 foci. The latter can only be the saddles in the polarization pattern of Fig. 4.

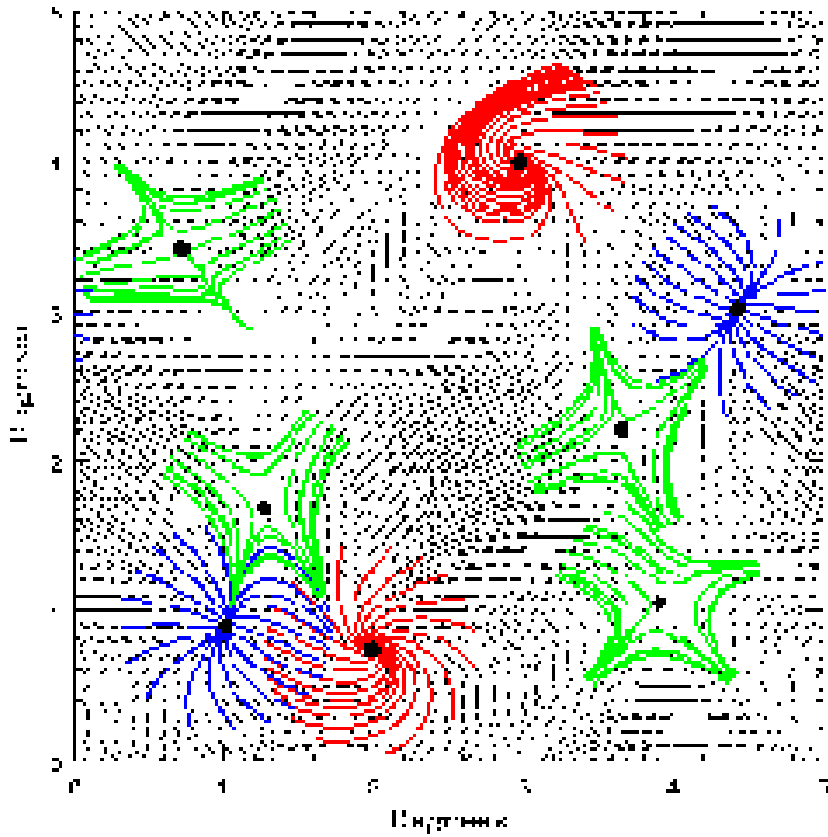


Figure 5: Simulated map of the flux lines of "vector" \vec{V} (see sec. 5 for details). Solid lines show the flux line behaviour near singular points where polarization vanishes.

6 Minkowski Functionals.

In this section we will consider an application of Minkowski Functionals (MF) for description of statistical properties of CMB polarization. For two dimensional maps the following three MF's are of interest: area (A), length (L), and genus (G). As usually, we will consider the magnitude of polarization, $\sqrt{Q^2 + U^2}$ as a two-dimensional surface in a three-dimensional space. If we cut this surface at different levels P_t , then the area of the map will be divided into two parts: the area where polarization is above the threshold P_t and the area where $P < P_t$. Three functions characterize this division:

1. "Area", A , is the fraction of the area of the map where $P > P_t$;
2. "Length", L , is the surface density of length of the boundary between the fractions with $P > P_t$ and $P < P_t$;
3. "Genus", G , is the number density of isolated highly polarized regions minus the number density of isolated weakly polarized regions (equivalent to the Euler characteristic).

All three Minkowski Functionals, A , L , and G , are evidently functions of P_t .

Minkowski Functionals (MF) have some mathematical properties that make them especially convenient for our task. They are translationally and rotationally invariant, additive, and have simple and intuitive geometrical meaning. Moreover, it was shown [22, 23] that morphological properties of any pattern in D -dimensional space, which possess the above mentioned characteristics, can be fully described by $D + 1$ Minkowski Functionals. The CMB polarization, that we consider, is a two-dimensional random field, so the introduced above three MF's would fully charac-

terize these properties. MF's are additive with respect to isolated parts of the sky that makes them potentially very powerful for patchy coverage. These properties make MF's a convenient tool for checking the polarization patterns for a presence of a non-Gaussian component.

For statistical analysis of CMB polarization field it is convenient to express the Stokes parameters Q and U in terms of scalar and pseudo-scalar potentials Ψ and Φ as given by eq. (12):

$$Q = \Phi_{11} - \Phi_{22} - 2\Psi_{12}, \quad U = 2\Phi_{12} + \Psi_{22} - \Psi_{22} \quad (50)$$

where Φ_{ij} , Ψ_{ij} are the second derivatives of Φ and Ψ in a Cartesian coordinate system in the small (flat) part of the sky, as is described above. The potentials Φ and Ψ can be considered as two independent two-dimensional Gaussian fields. For description of their statistical properties it is convenient to use their Fourier representation:

$$\begin{aligned} \Phi(\vec{x}) &= \frac{1}{2\pi} \int C_\Phi(k) e^{-i\vec{k}\vec{x}} d\vec{k} \\ \Psi(\vec{x}) &= \frac{1}{2\pi} \int C_\Psi(k) e^{-i\vec{k}\vec{x}} d\vec{k} \end{aligned} \quad (51)$$

Statistical properties of the fields Q , U and their derivatives are characterized by dispersions:

$$\begin{aligned} \sigma_Q^2 &= \frac{1}{2\pi} \left[\int_0^{2\pi} d\theta \cos^2(2\theta) \int_0^\infty k^5 |C_\Phi(k)|^2 dk + \int_0^{2\pi} d\theta \sin^2(2\theta) \int_0^\infty k^5 |C_\Psi^2(k)|^2 dk \right], \\ \sigma_U^2 &= \frac{1}{2\pi} \left[\int_0^{2\pi} d\theta \cos^2(2\theta) \int_0^\infty k^5 |C_\Psi(k)|^2 dk + \int_0^{2\pi} d\theta \sin^2(2\theta) \int_0^\infty k^5 |C_\Phi(k)|^2 dk \right], \\ \sigma_Q^2 &= \sigma_U^2 = \frac{1}{2} [\sigma_{0,\Psi}^2 + \sigma_{0,\Phi}^2], \\ \sigma_{0,\Phi}^2 &= \int_0^\infty k^5 |C_\Phi(k)|^2 dk, \quad \sigma_{0,\Psi}^2 = \int_0^\infty k^5 |C_\Psi(k)|^2 dk, \\ \sigma_{1,\Phi}^2 &= \int_0^\infty k^7 |C_\Phi(k)|^2 dk, \quad \sigma_{1,\Psi}^2 = \int_0^\infty k^7 |C_\Psi(k)|^2 dk, \\ \sigma_{2,\Phi}^2 &= \int_0^\infty k^9 |C_\Phi(k)|^2 dk, \quad \sigma_{2,\Psi}^2 = \int_0^\infty k^9 |C_\Psi(k)|^2 dk. \end{aligned} \quad (52)$$

Expressions for the correlators of first and second derivatives, namely, Q_i, Q_{ij}, U_i, U_{ij} , through $\sigma_{1,\Phi}^2, \sigma_{1,\Psi}^2, \sigma_{2,\Phi}^2$ and $\sigma_{2,\Psi}^2$, are presented below.

Two important characteristics of the polarization are the autocorrelation radius, r_c , and the coefficient of cross correlation between functions Q and U and their second derivatives, γ :

$$r_c^2 = \frac{\sigma_{0,\Psi}^2 + \sigma_{0,\Phi}^2}{\sigma_{1,\Psi}^2 + \sigma_{1,\Phi}^2}, \quad (53)$$

$$\gamma = \frac{\sigma_{1,\Psi}^2 + \sigma_{1,\Phi}^2}{(\sigma_{0,\Psi}^2 + \sigma_{0,\Phi}^2)^{1/2} (\sigma_{2,\Psi}^2 + \sigma_{2,\Phi}^2)^{1/2}}. \quad (54)$$

It is convenient to use instead of Q and U and their derivatives dimensionless variables, normalized to their dispersions:

$$\begin{aligned} q &= \frac{Q}{\sqrt{(\sigma_{0,\Psi}^2 + \sigma_{0,\Phi}^2) / 2}}, & u &= \frac{U}{\sqrt{(\sigma_{0,\Psi}^2 + \sigma_{0,\Phi}^2) / 2}}, \\ q_i &= \frac{Q_i}{\sqrt{(\sigma_{1,\Psi}^2 + \sigma_{1,\Phi}^2) / 2}}, & u_i &= \frac{U_i}{\sqrt{(\sigma_{1,\Psi}^2 + \sigma_{1,\Phi}^2) / 2}}, \\ q_{ij} &= \frac{Q_{ij}}{\sqrt{(\sigma_{2,\Psi}^2 + \sigma_{2,\Phi}^2) / 2}}, & u_{ij} &= \frac{U_{ij}}{\sqrt{(\sigma_{2,\Psi}^2 + \sigma_{2,\Phi}^2) / 2}}. \end{aligned} \quad (55)$$

Below we calculate Minkowski Functionals using these dimensionless variables. It is noteworthy that while $Q_i \equiv \partial Q / \partial x^i$, its dimensionless analogue, q_i , is not equal to $\partial q / \partial x^i$ but differs from it by the constant factor r_c . Thus, for example,

$$q_i = r_c \partial_i q, \quad q_{ij} = r_c^2 \partial_i \partial_j q \quad (56)$$

6.1 Area

The simplest Minkowski Functional, that is the fraction of area of the map with $p > p_t$, can be calculated using the joint probability distribution function (PDF)

$B(q, u)$ for values of q and u only. Since q and u are Gaussian fields, this function can be written using correlators for q and u and their dispersions:

$$\langle q \rangle = \langle u \rangle = \langle qu \rangle = 0, \quad \langle q^2 \rangle = \langle u^2 \rangle = 1 \quad (57)$$

and we have

$$B(q, u) dq du = \frac{1}{2\pi} \exp\left(-\frac{q^2}{2} - \frac{u^2}{2}\right) dq du, \quad (58)$$

The PDF of the amplitude $p = \sqrt{q^2 + u^2}$ is:

$$B(p) dp = p \exp\left(-\frac{p^2}{2}\right) dp \quad (59)$$

and the relative area of the map where $p > p_t$ is:

$$A(p_t) = \int_{p_t}^{\infty} B(p) dp = \exp\left(-\frac{p_t^2}{2}\right) \quad (60)$$

6.2 Length

The condition

$$p(x, y) = p_t \quad (61)$$

describes a curve in two-dimensional plane. The mean density of the length of this curve can be found from the expressions

$$dp(x, y) = (\nabla p \cdot d\vec{l}) = \sqrt{p_x^2 + p_y^2} \frac{dl}{r_c}, \quad (62)$$

$$L(p_t) = \frac{1}{r_c} \langle \sqrt{p_x^2 + p_y^2} \rangle B(p_t) \quad (63)$$

where $\langle \sqrt{p_x^2 + p_y^2} \rangle$ must be found for a given $p = p_t$.

To do this we should use the PDF $B(p_t, p_x, p_y)$. For Gaussian q and u this function would also have a Gaussian form and to find it we need correlators of q and u and their first derivatives:

$$\begin{aligned}
\langle qq_i \rangle &= \langle uu_i \rangle = \langle qu_i \rangle = \langle uq_i \rangle = 0, \\
\langle q_i \rangle &= \langle u_i \rangle = \langle q_i u_j \rangle = 0, \\
\langle q_i q_j \rangle &= \langle u_i u_j \rangle = \frac{1}{2} \delta_{ij}
\end{aligned} \tag{64}$$

where δ_{ij} is the Kronecker symbol. Using this correlators we obtain

$$B(p, p_x, p_y) dp dp_x dp_y = \frac{1}{\pi} p \exp\left(-p^2/2 - p_x^2 - p_y^2\right) dp dp_x dp_y, \tag{65}$$

$$\langle \sqrt{p_x^2 + p_y^2} \rangle = \frac{\sqrt{\pi}}{2} \tag{66}$$

and, finally,

$$L(p_t) = \frac{p_t \sqrt{\pi}}{2r_c} \exp\left(-\frac{p_t^2}{2}\right) \tag{67}$$

6.3 Genus

As is well known, Genus, $G(p_t)$ is expressed through the conditional mean value of determinant $\det(p_{ij}) = p_{11}p_{22} - p_{12}^2$ under conditions $p \geq p_t$, $p_i = 0$:

$$G(p_t) = \frac{1}{r_c^2} \int_{p_t}^{\infty} dp \int_{-\infty}^{\infty} \prod dp_{ij} \det(p_{ij}) B(p, p_i = 0, p_{ij}) = \frac{2}{\pi \gamma^2 r_c^2} \int_{p_t}^{\infty} dp B(p) \langle \Delta(p) \rangle \tag{68}$$

where $B(p, p_i = 0, p_{ij})$ is the conditional PDF of its arguments and $\langle \Delta(p) \rangle$ is the *conditional* mean of $\det(p_{ij})$. To find $\langle \Delta(p) \rangle$ we should know the *conditional* mean value and dispersions of p_{ij} which can be expressed through the *conditionless* mean value and non-vanishing correlators of q_{ij} and u_{ij} , namely:

$$\langle qq_{ii} \rangle = \langle uu_{ii} \rangle = -\frac{\gamma}{2} \delta_{ij},$$

$$\begin{aligned}
\langle q_{ii}^2 \rangle &= \frac{1}{16} \frac{7 + 5\rho^2}{1 + \rho^2}, \\
\langle u_{ii}^2 \rangle &= \frac{1}{16} \frac{5 + 7\rho^2}{1 + \rho^2}, \\
\langle q_{11}q_{22} \rangle &= \langle q_{12}^2 \rangle = \frac{1}{16} \frac{1 + 3\rho^2}{1 + \rho^2}, \\
\langle u_{11}u_{22} \rangle &= \langle u_{12}^2 \rangle = \frac{1}{16} \frac{3 + \rho^2}{1 + \rho^2}, \\
\langle q_{11}u_{12} \rangle &= \langle u_{11}q_{12} \rangle = \frac{1}{16} \frac{1 - \rho^2}{1 + \rho^2}, \\
\langle q_{22}u_{12} \rangle &= \langle u_{22}q_{12} \rangle = \frac{1}{16} \frac{-1 + \rho^2}{1 + \rho^2},
\end{aligned} \tag{69}$$

where $\rho^2 = \sigma_{2,\Psi}^2/\sigma_{2,\Phi}^2$. These correlators are linked to correlators p_{ij} through the expressions

$$p_{ij} = \frac{q}{p}q_{ij} + \frac{u}{p}u_{ij} + w_{ij}, \quad w_{ij} = \frac{1}{p}(q_iq_j + u_iu_j - p_ip_j) \tag{70}$$

The required determinant $\langle \Delta(p) \rangle$ can be written as

$$\begin{aligned}
\langle \Delta(p) \rangle &= \frac{q^2}{p^2} \langle q_{11}q_{22} - q_{12}^2 \rangle + \frac{u^2}{p^2} \langle u_{11}u_{22} - u_{12}^2 \rangle + \frac{qu}{p^2} \langle q_{11}u_{22} + u_{11}q_{22} \rangle \\
&\quad + \frac{q}{p} \langle w_{11}q_{22} + q_{11}w_{22} \rangle + \frac{u}{p} \langle w_{11}u_{22} + u_{11}w_{22} \rangle
\end{aligned} \tag{71}$$

and for *conditional* mean values we have

$$\begin{aligned}
\langle q_{11}q_{22} - q_{12}^2 \rangle &= \frac{\gamma^2}{4}(q^2 - 1), \\
\langle u_{11}u_{22} - u_{12}^2 \rangle &= \frac{\gamma^2}{4}(q^2 - 1), \\
\langle q_{11}u_{22} + u_{11}q_{22} \rangle &= 2\frac{\gamma^2}{4}qu, \\
\langle w_{11}q_{22} + q_{11}w_{22} \rangle &= -\frac{\gamma^2}{4}\frac{q}{p}, \\
\langle w_{11}u_{22} + u_{11}w_{22} \rangle &= -\frac{\gamma^2}{4}\frac{u}{p},
\end{aligned} \tag{72}$$

Finally

$$\begin{aligned} \langle \Delta(p) \rangle &= \frac{\gamma^2}{4}(p^2 - 3), \\ G(p_t) &= \frac{1}{2\pi r_c^2}(p_t^2 - 1)e^{-\frac{p_t^2}{2}} \end{aligned} \quad (73)$$

More cumbersome method for the calculation of the Genus was used in ref. [21] where the calculations have been done under incorrect assumptions about the correlations of p_{ij} . In spite of that, the final result obtained there remains true.

All three MF's have very simple analytical forms and can be used, together with other methods, to test the Gaussianity of CMB.

As was noted in ref. [31] and later discussed in refs. [21] and [19] the condition $G(p_{pr}) = 0$ defines the critical amplitude p_{pr} for which the regions of high polarization percolate. According to eq. (73) this critical amplitude of polarization is

$$p = p_{pr} = 1$$

that was tested in simulations made in ref. [21].

As has been mentioned above, $G(p_t)$ is equal to the number of isolated regions above p_t minus the number of isolated regions below p_t . For $p_t \ll 1$ the percolation takes place, $A \approx 1$ and almost all map is occupied by the one region with $p \geq p_t$. This means that only small isolated spots around the points $p = 0$ can be separated and the mean number density of such points, N_0 , is

$$N_0 = 1 - G(0) = \frac{1}{2\pi r_c^2} \quad (74)$$

As we can see from eqs. (53), (54) and (56) MF's have an universal form for any relation between the potentials Φ and Ψ . Therefore, Minkowski Functionals for the CMB polarization field do not depend on the type of perturbations and are determined

by the statistics of the signal only. To discriminate the scalar and pseudo-scalar perturbations and to estimate the parameter ρ given by eq. (69), a more detailed investigation of statistics of Q_{ij}, U_{ij} and p_{ij} needs to be performed. This implies, for example, direct estimates of some of the correlators (69) which would be a very difficult problem because of a finite resolution of the future polarization maps.

7 Summary and discussion

The main goal of this paper is to present a critical discussion of the known methods of analysis of statistical and geometrical properties of CMB polarization and to propose some new additional methods.

We have compared local and nonlocal descriptions of the polarization with different expressions for the field functionals S and P (see Sec. 3) in the case of noisy data. We conclude that the optimal observational strategy strongly depends upon the properties of the noise. For a sufficiently rare sources of noise on the sky, a measurement of local quantities S and P (7) which are obtained by differentiation of the Stokes parameters seems to be more favorable. However an isotropic noise with zero average may be easier to suppress by taking an average value over a part of the sky.

We established a classification of the singular points of the flux lines of the eigenvector $\vec{n}^{(+)}$ of the polarization (Stokes) matrix. We have found that there are three possible types of singularities at the points where polarization vanishes: saddles, comets, and beaks. They are different from the singularities known in the standard theory of two dimensional vector fields. The former, as is well known, are saddles, knots, and foci (even though the name "saddle" is the same in both cases the behavior of the flux lines are quite different). The reason for this difference is a square root

singularity of the vector $\vec{n}^{(+)}$ at the point where polarization vanishes. We have compared our method which was earlier presented in ref. [19] and described in detail here, with other methods [21, 15, 16].

It is shown that in the case of Gaussian primordial fluctuations (as predicted by inflationary cosmology) the saddles make 50% of all singular points, beaks make 5.2%, and comets make 44.8%. Deviations from these numbers may signal deviations from a Gaussian nature of perturbations or may indicate an existence of a non-Gaussian noise in observational data. We realize that a measurement of polarization near the points where it vanishes is a formidable observational problem. But the patterns on polarization maps created by the flux lines of $\vec{n}^{(+)}$ in the regions where polarization is non-zero is to a large extent determined by the types of nearest singularities. Thus one may hope that measurements of polarization on the patches where it is sufficiently large would permit to determine the singularity types.

Finally we applied Minkowski Functionals to the analysis of the statistic of the geometrical quantities on the polarization maps. It is shown that it provides a sensitive test of Gaussianity of CMB.

Acknowledgments

This work was supported in part by Danmarks Grundforskningsfond through its funding of the Theoretical Astrophysical Center (TAC), the Danish Natural Science Research Council through grant No 9401635, and in part by NSF-NATO fellowship (DGE-9710914) and by NSF EPSCOR program. D.N. thanks M. Kamionkowski for helpful discussions.

References

- [1] W. Hu, astro-ph/9508126.
- [2] W. Hu, N. Sugiyama, and J. Silk, Nature, **386**, 37 (1997); astro-ph/9604166.
- [3] J.R. Bond, in Proceedings of XXXI Moriond Conf., p.471, 1996; astro-ph/9610119.
- [4] M. Zaldarriaga, astro-ph/9806122.
- [5] C.R. Lawrence, D. Scott, and M. White, astro-ph/9810446.
- [6] W. Hu and M. White, New Astronomy, **2**, 323 (1997).
- [7] M.A. Basko and A.G. Polnarev, Sov. Astr. **24**, 3 (1979).
- [8] A.G. Polnarev, Sov. Astr. **29**, 607 (1985).
- [9] J.R. Bond, G. Efstathiou, Mon. Not. R. Astr. Soc. **226**, 655 (1987).
- [10] U. Seljak, Astrophys. J. **482**, 6 (1996); astro-ph/9608131.
- [11] U. Seljak and M. Zaldarriaga, Phys. Rev. Lett. **78**, 2054 (1997). astro-ph/9609169.
- [12] M. Zaldarriaga and U. Seljak, Phys. Rev D, **55**, 1830 (1997); astro-ph/9609170.
- [13] M. Kamionkowski, A. Kosowsky, A. Stebbins, Phys. Rev. Lett. **78** (1997) 2058; astro-ph/9609132.
- [14] M. Kamionkowski, A. Kosowsky, Phys.Rev. **D57** (1998) 685; astro-ph/9705129.
- [15] M. Kamionkowski, A. Kosowsky, and A. Stebbins, Phys. Rev. D, **55**, 7368 (1997); astro-ph/9611125.

- [16] U. Seljak and M. Zaldarriaga, astro-ph/9805010.
- [17] M. Kamionkowski, astro-ph/9803168.
- [18] M. Zaldarriaga and U. Seljak, astro-ph/9810257.
- [19] A.D. Dolgov, A.G. Doroshkevich, D.I. Novikov, and I.D. Novikov, TAC 1998-013, astro-ph/9806104.
- [20] G. Efstathiou and J.R. Bond, astro-ph/9807103, submitted to Mon. Not. R. Astr. Soc.
- [21] P.D. Naselsky and D.I. Novikov, *Astrophys. J.* **501**, 31 (1998); astro-ph/9801285.
- [22] H. Minkowski, *Mathematische Annalen*, **57** 447 (1903).
- [23] H. Hadwiger, *Vorlesungen über Inhalt, Oberfläche und Isoperimetrie*, Springer Verlag, Berlin, 1957.
- [24] S. Winitzki and A. Kosowsky, astro-ph/9710164.
- [25] J. Schmalzing and K.M. Gorski, astro-ph/9710185.
- [26] D. Novikov, H.A. Feldman, and S.F. Shandarin, astro-ph/9809238.
- [27] L. Popa, P. Stefanscu, and R. Fabbri , astro-ph/9812462.
- [28] A. Stebbins, astro-ph/9609149.
- [29] I.S. Gradshteyn and I.M. Ryzhik, *Tables of Integrals, Series, and Products*, Academic Press Inc. 1994.

- [30] I.N. Bronshtein, K.A. Semendyaev, *Spravochnik po matematike* (in Russian), Gostechizdat, Moscow, (1955). English translation: *Handbook of Mathematics*, Springer-Verlag, Berlin, Heidelberg, 1998.
- [31] K.R. Mecke and H Wagner, J. Stat. Phys. **64**, 843, (1991).